Synthesis and an investigation of the structural properties of Cu-Zn ferrite nanoparticles

Dr. Sabah M. Ali Ridha

University of Kirkuk / College of Education for Pure Sciences, Kirkuk, Iraq.
sabahyagmur@yahoo.com

Received 14 April 2014 ; Accepted 10 June 2014

Abstract

Ferrite nanoparticles with the spinel-type structures $Cu_{1-x}Zn_xFe_2O_4$ (where; x= 0.0 to 1.0) were synthesized using auto-combustion sol-gel method. Auto-combustion reaction temperature was determined by thermo-gravimetric analysis (TG), and found it is in the range of (200-220)°C. Fourier transform infrared spectra (FTIR) showed two absorption bands (ν_1 and ν_2) that are attributed to the stretching vibration of tetrahedral and octahedral sites in the spinel structure. X-ray diffraction was used to study the structural properties of the above investigated ferrites. Powder-forming particle sizes were characterized and calculated by XRD pattern peak (311) and scanning electron microscopy (SEM). As a result the average particle size found to be in the range of 15-30 nm. The lattice parameter (***a***) was calculated for each composition and it is in the range of (8.2733 to 8.3720 A°). A significant decrease in density and subsequent increase in porosity were observed with increasing Zn content in Cu-Zn ferrite.

Keywords: nanoparticles ferrites, Cu-Zn ferrite, magnetic materials, spinel ferrites.

الخصائص التركيبية لدقائق فرايت النحاس– زنك النانوي المحضرة بطريقة المحلول- الهلامي ذو الاحتراق الذاتي

د. صباح محمد علي رضا

جامعة كركوك / كلية التربية للعلوم الصرفة sabahyagmur@yahoo.com

الملخص

تاخذ القيم من الصفر الى x ذو التركيب السبنلي ($Cu_{1-x}Zn_xFe_2O_4$) حضرت دقائق نانوية لفيرايت النحاس– الزنك الواحد) بطريقة المحلول- الهلامي ذو الاحتراق الذاتي. تم تحديد درجة حرارة الاحتراق الذاتي بتقنية التحليل الحراري (TG) ووجدت بانها في المدى ٢٠٠ الى ٢٢٠ م°. طيف تحليل فورييه للاشعة تحت الحمراء (FTIR) اظهرت نطاقي امتصاص واضحتين (ν_1 و ν_2) واللتان تعودان للحزم الاهتزازية في الموقعين الرباعي والثماني ضمن التركيب السبنلي. استخدمت حيود الاشعة السينية (XRD) لدراسة الخصائص التركيبية للفرايت المحضر. تم فحص وحساب حجم جسيمات المسحوق من خلال القمة المميزة (٣١١) في طيف حيود الاشعة السينية وصورة المجهر الالكتروني الماسح (SEM). وكنتيجة لذلك تم الحصول على معدل حجم الجسيمات في المدى (١٥- ٣٠) نانومتر. ووجدت ان معلمة الشبيكة البلورية للفرايتات تقع في المدى (٨.٣٨٨٢–٨.٤٩٧٣) انكستروم. كما وتم ملاحظة تناقص في قيم الكثافة النظرية متبوعة بزيادة في المسامية مع زيادة محتوى الزنك في فيرايت النحاس – الزنك.

Synthesis and an investigation of the structural properties of Cu-Zn ferrite nanoparticles

Dr. Sabah M. Ali Ridha

الكلمات المفتاحية: فيرايتات ذو الدقائق رايت النحاس– الزنك ، المواد المغناطيسية، فرايتات ذو التركيب السبنلي النانوية،

1. Introduction

Spinel Ferrites possess the combined properties of magnetic materials and insulators. Nanocrystalline Ferrites represent an important class of functional magnetic materials, largely used in electronic industry and many other fields of interest, like high frequency devices, solid state physics, mobile communications of information technology, gas Sensors, and hyper-thermia for cancer treatment, etc.[1-4]. Ferrites has the structure of the mineral spinel corresponding to the general chemical formula $MeFe_2O_4$ where Me is a divalent ion of the transition elements and Fe is the iron trivalent ion Fe^{3+}. $CuFe_2O_4$ has inverse spinel structure with Cu^{2+} ions in octahedral sites and Fe^{3+} ions equally distributed between tetrahedral and octahedral sites whereas $ZnFe_2O_4$ has a normal spinel structure with Zn^{2+} ions in tetrahedral and Fe^{3+} in octahedral sites. Therefore, Zn-substitution in $CuFe_2O_4$ may have some distorted spinel structures depending upon the concentration of the precursor solutions [5]. Mixed ferrites have different degrees of inversion and Cu-Zn ferrites proved to be very sensitive to thermal treatments having different cation distribution depending upon annealing temperatures,[6].

Zn substituted Copper ferrites with a composition $Cu_{1-x}Zn_xFe_2O_4$ have been synthesized by one of the different methods like; double sintering ceramic, Sol-gel, Co-precipitation, Citrate, and Oxalate methods…etc., and characterized by X-ray diffraction,[7-10].

The present work deals with the synthesis of nanoparticles of zinc substituted copper ferrite ($Cu_{1-x}Zn_x Fe_2O_4$; where x= 0.0 to 1.0) via auto-combustion sol-gel method and characterized using Furrier Transform Infrared spectroscopy (FTIR), X-ray diffractometry (XRD). Studies were also carried out after sintering the samples at 1000°C for 3 hour with different Zn content to see the effect of Zinc content on bulk density and porosity of the ferrite samples. This work is an attempt to investigate the structural properties of zinc substituted copper ferrites.

2. Materials and methods

2.1. Sample preparation

A series of copper-zinc ferrite nanopowders with compositions of $Cu_{1-x}Zn_xFe_2O_4$ (where; x=0.0 to 1.0) were synthesized via sol–gel auto-combustion route. The detailed process can be described as follows, analytically pure (AR) grade Zn $(NO_3)_2{\cdot}6H_2O$ (mol. wt. 287.49 gm/mol), $Cu(NO_3)_2{\cdot}3H_2O$ (mol. wt. 241.60 gm/mol), and $Fe(NO_3)_3{\cdot}9H_2O$ (mol. wt. 404.00 gm/mol) as starting materials. Citric acid $C_6H_8O_7 \cdot H_2O$ (AR Grade, molecular weight: 210.14g/mol) was used as chelating agent. The appropriate amount of nitrates and citric acid as fuel was first dissolved into appropriate amount of de-ionized distilled water to form a mixed solution. The molar ratio of nitrates to citric acid is 1:1. Cold stirring was done on magnetic stirrer for 0.5 h to obtain homogeneous solution. The pH value of the mixture solution was adjusted to about (7) by adding ammonia solution. Then, the mixed solution was heated at 80°C under constant stirring to transform it into viscous brown gel. The resulting gel was dried in an oven at 120°C, then the dried gel was burnt at 220°C, this reaction was completed within a few seconds and loose powder was formed. The puffy, porous brown powders as-combusted was calcined at 600°C for 3 h with a heating rate of 10°C/minute.

For measuring the bulk density of the synthesized ferrites, the resulting powders were pressed into the pellet shape with Diameter =12mm and thickness=2mm by using metal dies. The

pressed products were finally sintered at 1000°C for 3 h with a heating rate of 10°C /min. The surfaces of all the samples were polished in order to remove any oxide layer which formed during the process of sintering.

2.2. Characterization

The structural characterization of the prepared ($Cu_{1-x}Zn_xFe_2O_4$) ferrite nanopowders was carried out using Philips X-ray diffraction system using Cu-Kα radiation (wave length λ= 1.54 A^o), while Crystal structure was determined from X-ray diffraction (XRD) data. The particle size D was calculated using most intense peak (311) employing the Scherer formula. The structural morphology is investigated using Scanning Electron Microscope (SEM). The FT–IR spectrum of ferrites nanoparticles was recorded in the range (4000–400 cm^{-1}).

The lattice constant ($a = b = c$) has been calculated from the most prominent peak (311) using the formula [11];

$$a = d\,(h^2+k^2+l^2)^{1/2} \qquad \ldots\ldots\ldots\ldots\ldots\ldots\ldots\ldots(1)$$

Crystallite size measurements: Crystallite size (D) was determined from the full-width at half maximum (FWHM) of the strongest reflection, the (311) peak using the Scherrer equation,[9];

$$D = k\lambda / \beta \cos\theta \qquad \ldots\ldots\ldots\ldots\ldots\ldots\ldots\ldots(2)$$

Where, D is the crystallite size of the synthesized nanoferrite, k is a shape function for which a value of 0.9 is used, and λ is the wavelength of the radiation (CuKa =0.154178 nm) and θ is the Bragg's angle. The value of (β) was determined from the experimental integral peak width (FWHM) by applying standard correction for the instrumental broadening,[11].

The x-ray density (d_x) of the Cu-Zn ferrite nanopowders has been calculated from the molecular weight and the volumes of the unit cell using the equation,[12];

$$d_x = 8M / Na^3 \qquad \ldots\ldots\ldots\ldots\ldots\ldots\ldots\ldots(3)$$

where, the factor 8 represents the number of molecules in a unit cell of spinel lattice, M is molecular weight, N is Avogadro's number and (**a)** is a lattice parameter. The porosity percentage was then calculated from d_B and d_X values using the expression [6];

$$P = \{1-(d_B / d_x)\}*100\ \% \qquad \ldots\ldots\ldots\ldots\ldots\ldots\ldots\ldots(4)$$

The bulk density d_B was measured by usual mass and dimensional consideration of the ferrite samples sintered at 1000°C for 3 h..

3. Results and discussion

Copper-Zinc ferrite nanopowders were synthesized via auto-combustion sol-gel route. It is well known that during the auto-combustion reaction the process of oxide formation involves liberation of gaseous products, which is accompanied by a decrease of mass. Thus, thermogravimetry (TG) of the corresponding ferrite determined as in figure (1).The auto-combustion initiation temperature of dry gel is found to be in the range of 200–220 °C.

Synthesis and an investigation of the structural properties of Cu-Zn ferrite nanoparticles

Dr. Sabah M. Ali Ridha

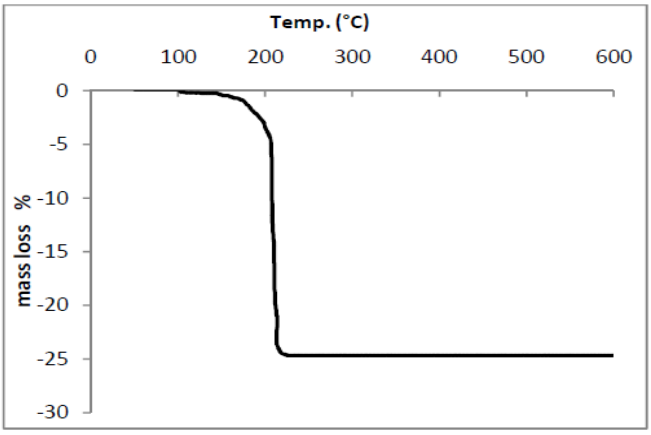

Figure (1): TG curve of dried gels for Cu-Zn ferrite

FTIR spectra of the synthesized $Cu_{1-x}Zn_xFe_2O_4$ ferrite nanoparticles (with x=0 and 0.1) in the range of 400 to 4000 cm^{-1} are shown in Figure (2). Two strongest absorption bands ($\boldsymbol{\nu_1}$ and $\boldsymbol{\nu_2}$) are observed at the ranges 406-412 and 570-579 cm^{-1}, respectively. These bands are attributed to the stretching vibration due to interactions between the oxygen atom and the cations in tetrahedral and octahedral sites, respectively. The difference between $\boldsymbol{\nu_1}$ and $\boldsymbol{\nu_2}$ is due to the changes in bond length (Fe-O) at the octahedral and tetrahedral sites.

The main absorption bands at 570 & 579 cm^{-1}($\boldsymbol{\nu_1}$) for x=0 & x=0.1, respectively were attributed to stretching vibration of tetrahedral sites, while the bands at 406 and 412 cm^{-1}($\boldsymbol{\nu_1}$) for x=0 and x=0.1, respectively related to the octahedral sites. The $\boldsymbol{\nu_1}$ band was changed to higher frequency with progressive doping of Zn ions due to stretching of Fe-O bonds.

FTIR spectra show that the Zn^{+2} ions occupy the tetrahedral site, while Cu^{2+} ions occupy the octahedron sites and some fraction of tetrahedron sites. As shown in figure (2), the absorption broad band at 3410 cm^{-1} represents the stretching mode of OH group which is assigned to surface OH groups of Cu-Zn ferrite nanoparticles and indicating that the powders have absorbed large amount of water. The band at 1400-1500cm^{-1} is ascribed to a symmetric stretching vibration appearing from the residual nitrate, while asymmetrical stretching vibrations are observed at the band 1560-1640 cm^{-1}.

Synthesis and an investigation of the structural properties of Cu-Zn ferrite nanoparticles

Dr. Sabah M. Ali Ridha

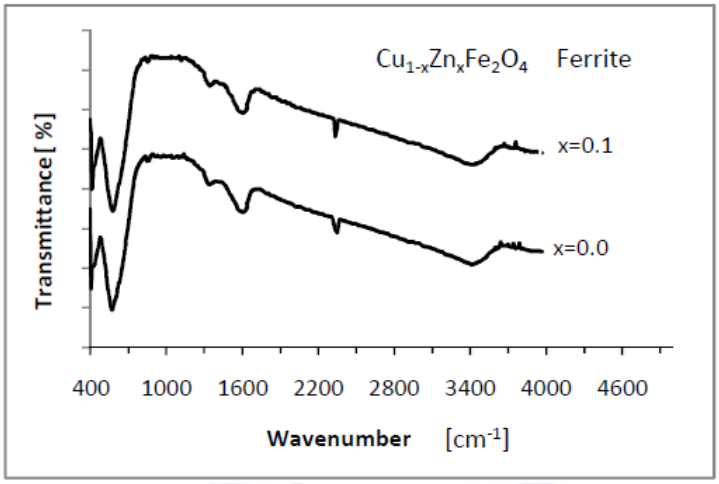

Figure (2): FTIR spectrum of Cu-Zn ferrite nanoparticles.

Figure (3) represents the x-ray powder diffraction pattern of synthesized $Cu_{1-x}Zn_xFe_2O_4$ ferrite samples annealed at 600°C (where, x= 0.0 - 1.0). The pattern shows different reflection planes indexed as (111), (220), (311), (222), (400), (511) and (440), which are in a good agreement with the standard XRD pattern, JCDPS card no. (00-25-0283).These patterns showing well-defined reflections without any ambiguity, exhibits the formation of a single-phase cubic spinel structure. The XRD patterns in figure (3) reveals that the diffraction peaks became broader with increasing Zn content x, which may be attributed due to the reduced nanocrystallite size with Zn doping. As a result, the mean particle size was found in the range 0f (19–27.7nm) calculated from the peak (311) of the XRD diffractogram employing by Scherrer's formula**.** The right side of figure (3) shows the XRD pattern most intense peak (311) of the Cu-Zn ferrite powders with different Zn content (x). It can be clearly observed that the diffraction peak (311) became broader and shifts toward smaller angles with increasing Zn content and it results in the decrease of particle size.

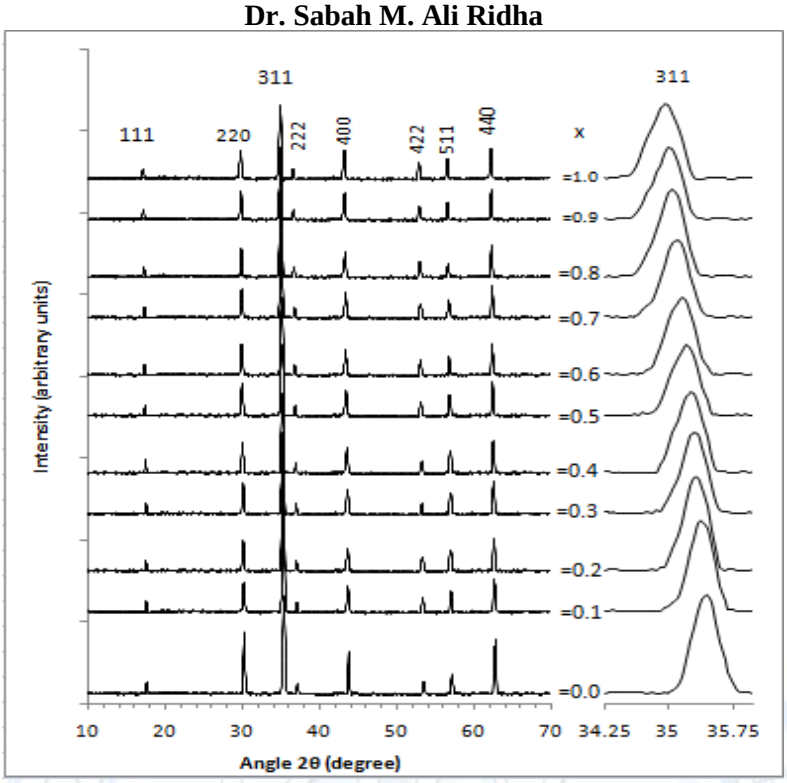

Fig. (3): (left side) shows the XRD pattern indicating (hkl) values of each peak of $Cu_{1-x}Zn_xFe_2O_4$ ferrite nanopowders (x values from 0.0 to 1.0) , and (right side) shows the shifting of the (311) peak with deferent x values.

By using the XRD patterns peak (311) of the Cu-Zn ferrite powders, experimental parameters (FWHM, particle size **D**, lattice parameter **a** , x-ray density $\mathbf{d_x}$, bulk density $\mathbf{d_B}$ and porosity **P**) were calculated using the equations (1 to 4) and the results are listed in table (1). The observed particle size of $Cu_{1-x}Zn_xFe_2O_4$ ($0.0 \leq x \leq 1.0$) is listed in Table (1). Furthermore, it is observed that the particle size **D** decreases with increasing Zn content and is plotted as shown in the Figure 4(a) .This figure observes that the FWHM increases with increasing Zn content and it results in the decrease of particle size. This effect may be due to the reaction time and temperature during the synthesis process. Figure 4(b) shows the variation of lattice constant with Zn content. A linear increase was observed in the lattice constant with increasing Zn content from 8.2733 to 8.3720 Å. This increase can be attributed to the ionic size differences since the unit cell has to expand when substituted by ions with large ionic size. The ionic radius of Zn^{2+} ions (R_{Zn+2} = 0.82 Å) is larger than that of Cu^{2+} ions (R_{Cu2+} = 0.70 Å), [13].

Table (1): Experimental parameters (FWHM, particle size, lattice parameter, x-ray density, bulk density, porosity, and lattice strain) calculated using XRD pattern peak (311) characteristics of $Cu_{1-x}Zn_xFe_2O_4$ ferrite nanopowders.

Zn content (x)	FWHM Of (311) peak (β) degree.	(2θ) angle center of (311) peak (degree)	Particle size D (nm)	Lattice constant a (A°)	x-ray density d_x (g/cm^3)	Bulk density d_B (g/cm^3)	Porosity % P
0.0	0.300	35.35	27.79	8.2733	5.6122	5.164	7.987
0.1	0.310	35.3	26.89	8.2846	5.5935	5.067	9.413
0.2	0.322	35.25	25.89	8.2960	5.5748	4.989	10.508
0.3	0.340	35.2	24.51	8.3074	5.5561	4.894	11.917
0.4	0.355	35.18	23.47	8.3120	5.5512	4.848	12.667
0.5	0.363	35.14	22.95	8.3212	5.5371	4.815	13.041
0.6	0.371	35.12	22.45	8.3258	5.5322	4.79	13.415
0.7	0.380	35.1	21.92	8.3304	5.5272	4.76	13.881
0.8	0.397	35.06	20.98	8.3396	5.5131	4.73	14.205
0.9	0.410	35.01	20.31	8.3511	5.4945	4.7	14.460
1.0	0.433	34.92	19.23	8.3720	5.4577	4.68	14.250

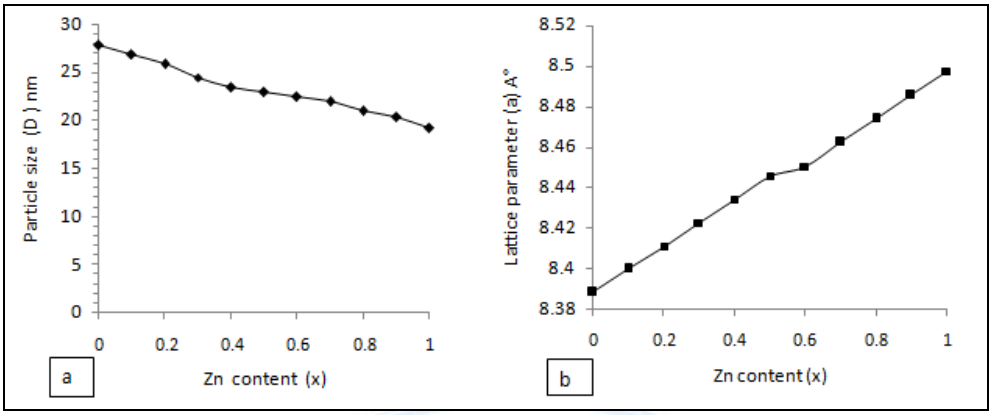

Figure (4) : part (a) shows the particles size of the Cu-Zn ferrite nanopowders as a function of the Zn content (x), and the part (b) shows Lattice parameter vis Zn content in the Cu-Zn ferrite nanopowders

Figure (5) shows SEM images of typical $Cu_{1-x}Zn_xFe_2O_4$ (at x=0.1 and 0.9) nanoparticles annealed at temperature 600°C. As can be seen in Figure a(a) and (b), the powders exhibit a compact arrangement of homogenous nanoparticles with spherical shape for $Cu_{0.9}Zn_{0.1}Fe_2O_4$ and $Cu_{0.1}Zn_{0.9}Fe_2O_4$ ferrite nanopowders respectively. According to these micrographs, the microstructure is mainly influenced by the Zn content in Cu-Zn ferrite. It is observed that the porosity affects the physical properties of the prepared ferrites. The nanoparticles are equally distributed and the measurement of particle size is clear. As a result the average particle size found to be in the range of 15-30 nm. Therefore the observed particles size from the XRD measurements is well in agreement with SEM analysis.

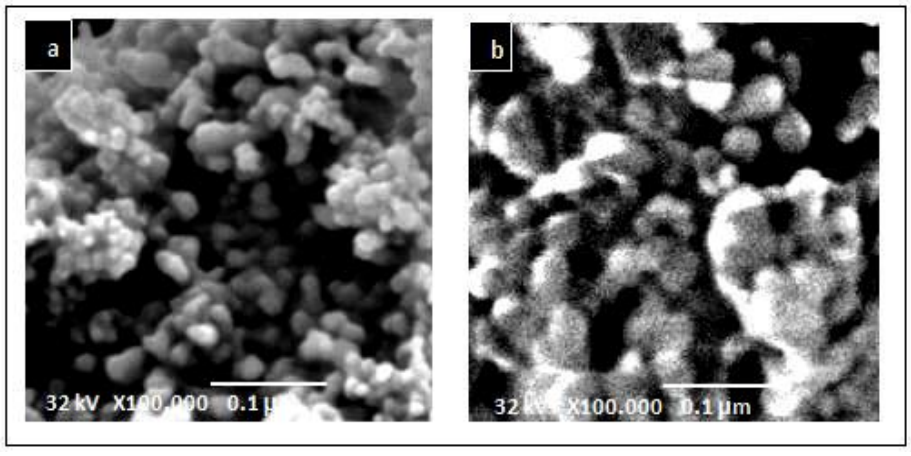

Figure (5): SEM images of $Cu_{1-x}Zn_xFe_2O_4$ ferrite nanopowders annealed at 500 °C for (a): x=0.1 and (b): x= 0.9

The variation of XRD and bulk densities (d_x and d_B) is shown in Fig. 6(a). By increasing Zn content (x) in Cu-Zn ferrite, a decrease of X-ray and bulk densities is observed. The X-ray density depends upon the lattice parameters and molecular weight of the ferrite composition. As lattice constants increase linearly with the increase of Zn content, X-ray density decreased. Figure 6(a) shows that the X-ray densities are larger in magnitude than that of bulk densities; this may be due to the existence of pores which were formed and developed during the ferrite preparation or the thermal process.

The effect of Zn content on the porosity is shown in Table (1) and Figure 6(b). Porosity is found to be increased from 7.9% to 14.25% for x = 0.0 and x=1, respectively. As a result the porosity in all samples is not exceeds 14.25% and this indicates the existence of few pores in the prepared ferrites.

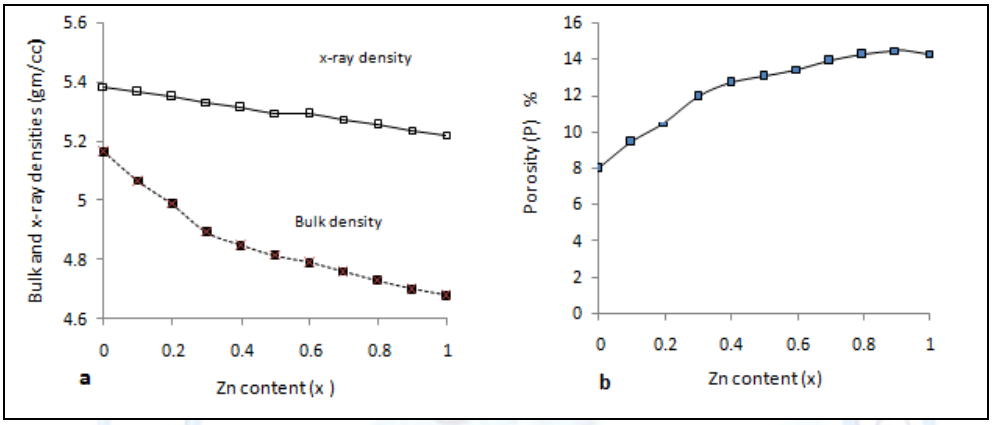

Figure (6):(a); X-ray and bulk densities with Zn content, and (b); porosity with Zn content for Cu-Zn nanoferrite.

4. Conclusions

The substitution of Zn ions in $Cu_{1-X}Zn_XFe_2O_4$ ferrite causes appreciable changes in its structural and physical properties. FTIR spectra showed two absorption bands (ν_1 and ν_2) that are attributed to the stretching vibration of tetrahedral and octahedral sites. XRD pattern peak (311) position shifts to the smallest angles (2θ) with increasing Zn content. All ferrites have existence of single phase cubic spinel structure with the decrease of x-ray density, particle size and bulk density whereas increase porosity with increasing Zn contents. The lattice parameter is found to be increased linearly with increasing Zn content.

References

[1] Raul V. "Magnetic ceramics" Cambridge University Press, New York, USA, 1994.

[2] Cullity B. D. and Graham C. D. 'Introduction to magnetic materials" 2nd Edition, Published by John Wiley & Sons, Inc., Hoboken, New Jersey, 2009

[3] Challa S. S. R. Kumar and Faruq Mohammad,"magnetic nonmaterial's for Hyperthermia-based Therapy and controlled Drug delivery" Advanced Drug delivery review, Vol. 63, Issue 9, pp. 789-808, 14 August 2011.

[4] Jagtap S. V. , Kadu A. V., Gedam N. N. and Chaudhari G. N., "Ammonia Gas Sensing Properties of Nanocrystalline $Zn_{1-x}Cu_xFe_2O_4$ Doped with Noble Metal" Sensors & Transducers Journal, Vol. 122, Issue 11, pp. 120-127 , November 2010.

[5] Gerald F. Dionne "Magnetic Oxides" Springer New York Dordrecht Heidelberg London,2009

[6] Standley K., "Oxide Magnetic Materials," 2nd Edition, Clarendon, Oxford, p. 97, 1974.

[7] Shahida A., Deba P. P., M. A. Hakim, Dilip K. S., Al-Mamun M.,and Alhamra P." Synthesis, Structural and Physical Properties of $Cu_{1-x}Zn_xFe_2O_4$ Ferrites " Materials Sciences and Applications, Vol. 2, No.11 pp. 1675-1681, Nov.16, 2011.

[8] Fatemeh Z., **Ta**ghi D. Isfahani, and Iraj H." Hydrothermal synthesis of copper ferrite nanoparticles by sodium citrate synthetic process" Proceedings of the 4th International Conference on Nanostructures (ICNS4), 12-14 March, 2012, p.p.1394-1396, Kish Island, I.R. Iran.

[9] Anuj J., Ravi K. B., Ajaya B., Vakil Z., and Prajapati C. S. " Study of Zn-Cu Ferrite Nanoparticles for LPG Sensing" The Scientific World Journal, Vol. 2013, p.p.1-7, 2013

[10] Hankare P. P., Jadhav S.D., Sankpal U. B., Patil R. P., Sasikala R., and Mulla I. S., "Gas sensing properties of magnesium ferrite prepared by co-precipitation method," Journal of Alloys and Compounds, Vol. 488, No. 1, pp. 270–272, 2009.

[11] Cullity B. D., "Elements of X-ray Diffraction" Addison-Wesley Publishing Company, p. 101, 1978.

[12] Kazi H. Maria, Shamima C., and Mohammad A. Hakim,"Structural phase transformation and hysteresis behavior of Cu-Zn ferrites" International Nano Letters , Vol. 3, pp. 1-10, 2013.

[13] Lionel M. Levinson, "Electronic ceramics; properties, devices and application", Marcel Dekker, INC., New York, USA, p.156, 1988.